Ceramics International xxx (xxxx) xxx–xxx

Contents lists available at ScienceDirect

Ceramics International

journal homepage: www.elsevier.com/locate/ceramint

Bond ionicity, lattice energy, bond energy, and microwave dielectric properties of $Ca_{1-x}Sr_xWO_4$ ceramics

Mi Xiao*, Hongrui Sun, Ziqi Zhou, Ping Zhang*

School of Electrical and Information Engineering & Key Laboratory of Advanced Ceramics and Machining Technology of Ministry of Education, Tianjin University, Tianjin 300072, PR China

ARTICLE INFO

Keywords:
Microwave properties
Bond iconicity
Lattice energy
Bond energy

ABSTRACT

The $Ca_{1-x}Sr_xWO_4$ (x = 0, 0.02, 0.04, 0.06, 0.08, 0.10) ceramics were fabricated through solid-state reaction, and the relationships among microwave dielectric properties of $Ca_{1-x}Sr_xWO_4$, bond ionicity, lattice energy and bond energy were systematically investigated for the first time. The patterns of X-ray diffractions of $Ca_{1-x}Sr_xWO_4$ presented tetragonal scheelite structure and no second phase appeared throughout the entire compositions. Dielectric properties of $Ca_{1-x}Sr_xWO_4$ were proved to be related to the microstructures: dielectric constant (ε_r) of $Ca_{1-x}Sr_xWO_4$ was dependent on the bond ionicity; the quality factor ($Q\times f_0$) of $Ca_{1-x}Sr_xWO_4$ was affected by W-site lattice energy when intrinsic loss is dominant; the temperature coefficient of resonant frequency ($|\tau_f|$) would increase if B-site bond energy decreased. $Ca_{1-x}Sr_xWO_4$ ceramic showed excellent microwave dielectric properties, ε_r = 9.42, $Q\times f_0$ = 79876 GHz and τ_f = −18.8 ppm/°C when x = 0.08 and sintered at 1100 °C for 4 h.

1. Introduction

Microwave dielectric ceramics play important roles in the development of global positioning systems, satellite broadcasting and 5 G resonators [1–3]. And the excellent microwave properties will effectively make devices smaller and improve the packaging density of the microwave integrated circuits [4]. Research on new microwave dielectric ceramics with high dielectric constant (ε_r), high quality factor ($Q\times f_0$) and near-zero temperature coefficient of resonant frequency (τ_f) has become a hotspot.

The tetragonal scheelite structure material $CaWO_4$ with ε_r = 10.40, $Q\times f_0$ = 76,550 GHz, τ_f = -22.4 ppm/°C was firstly reported by Kim et al. [5] Owing to its high $Q\times f_0$ value and low sintering temperature (1100 °C), the $CaWO_4$ is regarded as a kind of promising material for microwave applications. Some efforts have been made in recent years to decrease the sintering temperature and improve dielectric properties to meet the application requirements. $CaWO_4$ ceramics modified with $Na_2W_2O_7$ were reported by Wang et al., which can be densified at 850 °C for 2 h, meanwhile, its microwave dielectric properties were not affected greatly if the amount of $Na_2W_2O_7$ was appropriate [6]. (1-x)$CaWO_4$-xLi_2WO_4 ceramics were also investigated to decrease the sintering temperature, and presented outstanding microwave dielectric properties: ε_r= 9.00, $Q\times f_0$ = 117,600 GHz and τ_f= −55.0 ppm/°C when x = 0.1, and the sintering temperature were successively reduced to 900 °C [7]. Moreover, people also made attempt to improve the microwave dielectric properties by substitution. Xiao et al. revealed the effect of Mo^{6+} substitution at Ca-site on $Ca(W_{1-x}Mo_x)O_4$ ceramics, and the dielectric constant (ε_r) increased slightly with MoO_3. The optimum microwave dielectric properties were achieved when x = 0.06: ε_r = 10.22, $Q\times f_0$ = 79,919 GHz and τ_f = -40.4 ppm/°C [8]. Zhou et al. [9] studied the microwave dielectric properties of $[(Li_{0.5}Ln_{0.5})_{1-x}Ca_x]MoO_4$ (Ln=Sm and Nd), and found that a near-zero temperature coefficient of resonant frequency can be obtained at x = 0.80 and 0.85 for $[(Li_{0.5}Sm_{0.5})_{1-x}Ca_x]MoO_4$ and $[(Li_{0.5}Nd_{0.5})_{1-x}Ca_x]MoO_4$ solid solutions, respectively.

In this paper, bond ionicity, lattice energy and bond energy were calculated based on complex chemical bond theory [10]. The relationships among bond ionicity, lattice energy, bond energy, and microwave dielectric properties of $Ca_{1-x}Sr_xWO_4$, ceramics were discussed.

2. Experimental procedure

The ceramics were prepared by the traditional solid-state method. High-purity powders of $CaCO_3$ (99.9%), WO_3 (99.9%), $SrCO_3$ (99.9%) were used as the starting materials. The raw materials were weighted according to the formula $Ca_{1-x}Sr_xWO_4$ (x = 0, 0.02, 0.04, 0.06, 0.08, 0.10). Then the mixed powders were ball milled for 8 h with ZrO_2 balls and absolute alcohols in a nylon container. Then the slurries were dried

* Corresponding author.
E-mail addresses: xiaomi@tju.edu.cn (M. Xiao), zhangping@tju.edu.cn (P. Zhang).

https://doi.org/10.1016/j.ceramint.2018.08.062
Received 25 May 2018; Received in revised form 22 July 2018; Accepted 7 August 2018

and pre-sintered at 700 °C for 2 h. The pre-sintered powders were ball-milled for another 8 h with absolute alcohol. After dried, the powders were pressed into cylinders with 10 mm in diameter and 5 mm in height under the pressure of 10 MPa. These cylinders were sintered at 1100 °C for 4 h in air with a heating rate of 5 °C/min.

Crystalline phases of the specimens were identified by the powder X-ray diffraction analysis (XRD, Rigaku D/max 2550 PC, Tokyo, Japan). The surfaces of ceramics were observed by scanning electron microscopy (SEM, MERLIN Compact, Germany). A network analyzer (N5234A, Agilent Co, America) was used for the measurement of microwave dielectric properties. The temperature coefficients of resonant frequency (τ_f) were measured in the range from 25 °C to 85 °C. The τ_f (ppm/°C) value was calculated by Eq. (1).

$$\tau_f = \frac{f_2 - f_1}{f_1(T_2 - T_1)} \tag{1}$$

where f_1 is the resonant frequency at T_1 (25 °C) and f_2 is the resonant frequency at T_2 (85 °C).

3. Results and discussion

3.1. Microstructure analysis

The X-ray diffraction patterns of $Ca_{1-x}Sr_xWO_4$ (x = 0.0, 0.02, 0.04, 0.06, 0.08, 0.10) ceramics sintered at 1100 °C are shown in Fig. 1. All the patterns are matched well with ICSD file No. 15586, which indicates pure single-phase of tetragonal scheelite structure was obtained in all the samples. The patterns around 29°are enlarged in the insets in Fig. 1, from which we can see that the angles of the diffraction peaks shift for the lower direction with the increase of x, which means the more the substitution amount of Sr^{2+} for Ca^{2+}, the larger the unit-cell volume. The reason is the radius of Sr^{2+} (r = 1.16 Å, CN = 6) is larger than that of Ca^{2+} (r = 1.00 Å, CN = 6).

Surface morphologies of the $Ca_{1-x}Sr_xWO_4$ samples are shown in Fig. 2. The grains' size increased with the substitution amount of Sr^{2+}. The samples were all well-sintered and no obvious pore was found in the surface of the samples.

Surface morphologies of the $Ca_{1-x}Sr_xWO_4$ samples are shown in Fig. 2. The grains' size increased with the substitution amount of Sr^{2+}. However, obvious pores were found in the surface of the samples when the substitution amount of Sr^{2+} was 0.10.

3.2. Multiphase refinement

In order to analyze the effects of different substitution amount on lattice parameter, the major structure parameters, such as zero point, background, half-width, asymmetry parameters, unit-cell parameters, atomic positional coordinates were refined using the software of FullProf. The results are acceptable when the Rietveld discrepancy factors R_p and R_{wp} are lower than 15%.

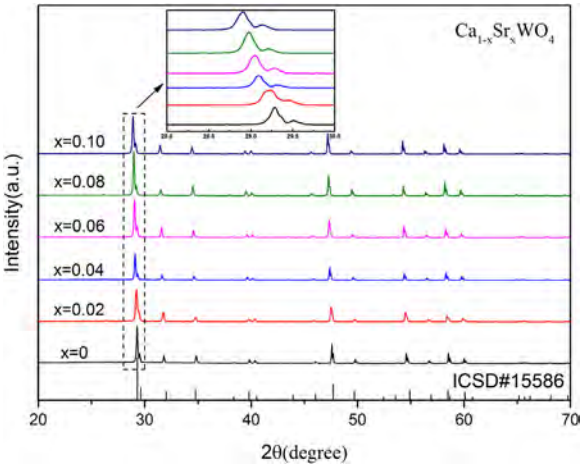

Fig. 1. The XRD patterns of $Ca_{1-x}Sr_xWO_4$ (x = 0.0, 0.02, 0.04, 0.06, 0.08, 0.10) ceramics sintered at 1100 °C for 4 h.

The cell parameters and bond-length obtained after refinement are shown in Table 1. The volume of the unit cell increases slightly, which is consistent with the X-ray diffraction results shown in Fig. 1.

3.3. Bond ionicity, lattice energy and bond energy calculation

According to the chemical bond theory, the values obtained by the Rietveld refinement could be used to calculate the bond ionicity, lattice energy and bond energy which are related to the microwave dielectric properties of $Ca_{1-x}Sr_xWO_4$ ceramics. The analyses about them are following.

3.3.1. Complex chemical bond theory and disassembly of $CaWO_4$ bonds

Fig. 3 shows the schematic of crystal structure of $CaWO_4$. The microstructure of $CaWO_4$ consists of tetrahedrons with a W^{6+} ion at the center and O^{2-} ions at vertexes. Ca^{2+} are surrounded by eight O^{2-}, and an O^{2-} is with two Ca^{2+} and one W^{6+} as the nearest neighbor.

Based on the Phillips-Van (PV) theory [11], the binary crystals can be decomposed [12–14]. Complex crystal could be disassembled into binary crystals.

$$A_{a1}^1 A_{a2}^2 \ldots A_{ai}^i \ldots B_{b1}^1 B_{b2}^2 \ldots B_{bj}^j = \sum_{ij} A_{mi}^i B_{nj}^j \tag{2}$$

where A^i and B^j are different symmetric sites of different elements or the same element, respectively.

According to the chemical bond theory mentioned above and the information of the crystal structure, the $CaWO_4$ can be decomposed into binary crystals as follow [15]:

$$CaWO_4 = CaO_{8/3} + WO_{4/3}$$

The effective valence electron number of each ion is significant for the analysis and calculation of the lattice energy. In the $CaWO_4$ ceramic, the numbers of effective valence electron of Ca^{2+} and W^{6+} are 2 and 6, respectively. Accordingly, the effective valence electron numbers of O^{2-} are: Z_O = -0.75 in Ca-O bond, and Z_O = -4.5 in W-O bond.

3.3.2. Calculation of the bond ionicity

The bond ionicity f_i and bond covalency f_c, which are the two opposite aspects of bond property, can be calculated as follow:

$$f_i = \frac{(C^\mu)^2}{(E_g^\mu)^2} \tag{3}$$

$$f_c = \frac{(E_h^\mu)^2}{(E_g^\mu)^2} \tag{4}$$

where E_g^μ is the average energy gap and can be defined as follows:

$$(E_g^\mu)^2 = (E_h^\mu)^2 + (C^\mu)^2 \tag{5}$$

where E_h^μ and C^μ represent the homopolar and heteropolar parts for binary crystal A_mB_n type compounds, and can be calculated by following:

$$(E_h^\mu)^2 = \frac{39.74}{(d^\mu)^{2.48}} \tag{6}$$

$$C^\mu = 14.4 b^\mu e^{(-k_s^\mu r_o^\mu)} \left[\frac{(Z_A^\mu)^*}{r_o^\mu} - \frac{n}{m} \frac{(Z_B^\mu)^*}{r_o^\mu} \right] \left(\text{if } n > m \right) \tag{7}$$

$$C^\mu = 14.4 b^\mu e^{(-k_s^\mu r_o^\mu)} \left[\frac{m}{n} \frac{(Z_A^\mu)^*}{r_o^\mu} - \frac{(Z_B^\mu)^*}{r_o^\mu} \right] \left(\text{if } n < m \right) \tag{8}$$

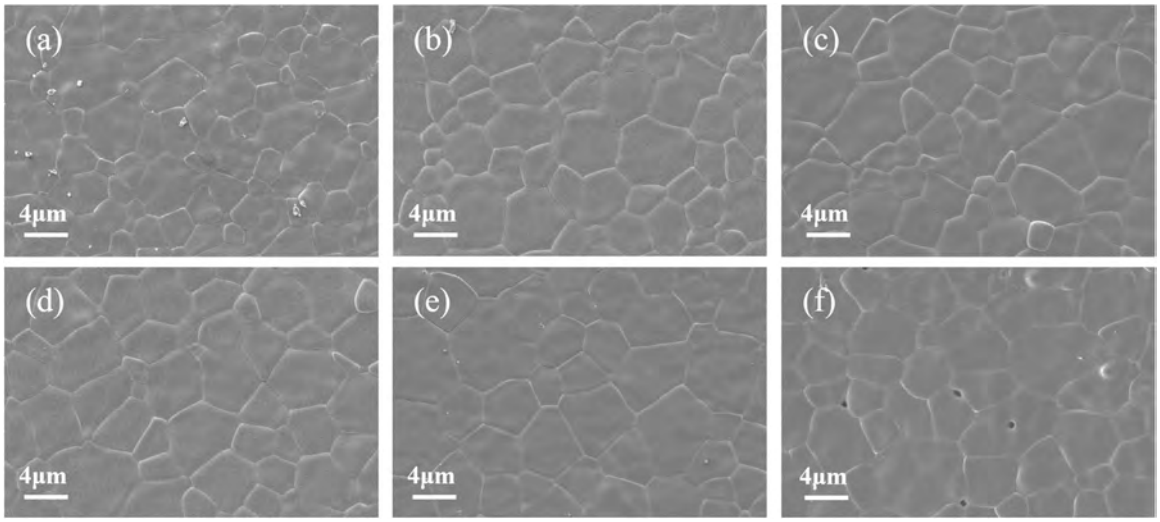

Fig. 2. The SEM of the $Ca_{1-x}Sr_xWO_4$ sintered at 1100 °C for 4 h: x = 0.0, (b) x = 0.02, (c) x = 0.04, (d) x = 0.06, (e) x = 0.08, (f) x = 0.10.

Table 1
Crystallographic data after Rietveld refinement of $Ca_{1-x}Sr_xWO_4$ ($0 \leq x \leq 0.10$) ceramics.

x	a(Å)	b(Å)	c(Å)	V_{cell}(Å^3)	R_p(%)	R_{wp}(%)	$d_{Ca\text{-}O(1)}$	$d_{Ca\text{-}O(2)}$	$d_{W\text{-}O}$
0	5.2515	5.2515	11.4058	314.55	11.9	10.8	2.3292	2.3319	1.9836
0.02	5.2563	5.2563	11.4069	315.16	11.9	10.9	2.3306	2.3443	1.9810
0.04	5.2618	5.2618	11.4125	315.97	11.5	10.3	2.3329	2.3470	1.9797
0.06	5.2675	5.2675	11.4186	316.83	12.2	10.9	2.3375	2.3498	1.9780
0.08	5.2709	5.2709	11.4218	317.32	11.5	10.7	2.3418	2.3524	1.9760
0.10	5.2758	5.2758	11.4269	318.06	11.4	11.0	2.3458	2.3543	1.9735

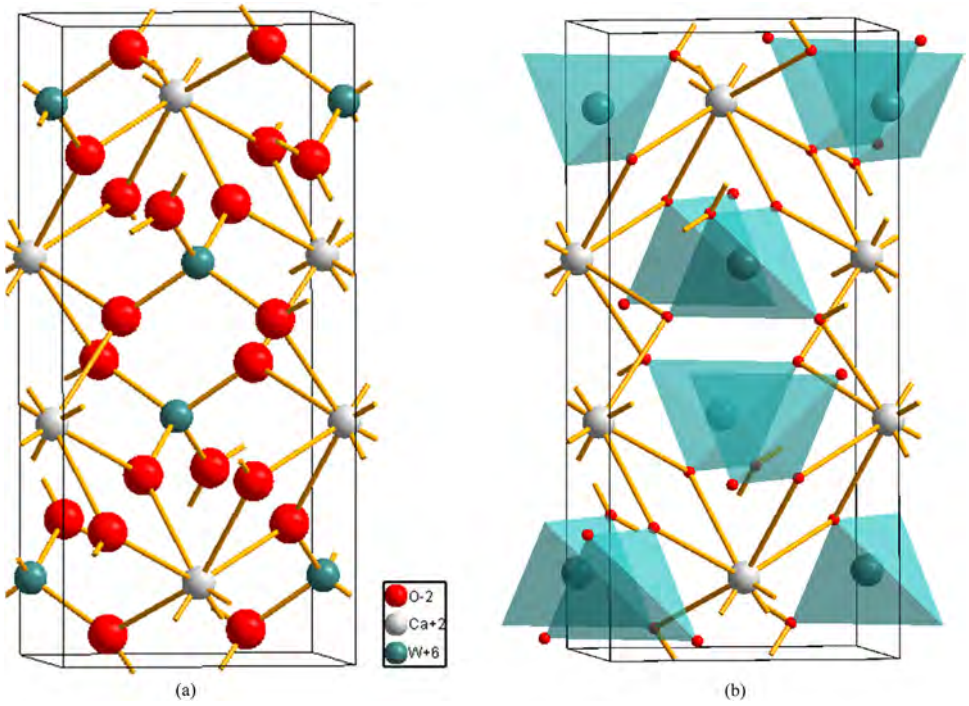

Fig. 3. Crystal structure of $CaWO_4$: (a) the coordination number of ions in $CaWO_4$, (b) the unit cell of $CaWO_4$.

where d^{μ} is the bond length. $(Z_A^{\mu})^*$ and $(Z_B^{\mu})^*$ represent the effective numbers of valence electrons on the cation A and the anion B, and b is the correction factor which correlates with the average coordination number.

The calculation results of bond ionicity f_i (%) are shown in Table 2.

3.3.3. Calculation of the lattice energy

The lattice energy reflects combining force in crystal and the crystal will be stable at larger lattice energy. U_{cal} is the sum of U_b^{μ}. The lattice energy U_{cal} can be divided into two parts, U_{bc}^{μ} and U_{bi}^{μ}, which are the covalent part and ionic part of μ bond respectively.

Table 2
Bond ionicity f_i for $Ca_{1-x}Sr_xWO_4$ ceramics.

x	Bond ionicity f_i (%)		
	Ca-O(1)	Ca-O(2)	W-O
0	75.8012	75.8658	68.8595
0.02	75.8044	75.8897	68.8325
0.04	75.8220	75.8973	68.8122
0.06	75.8422	75.9076	68.7832
0.08	75.8593	75.9154	68.7617
0.10	75.8747	75.9195	68.7493

Table 3
Lattice energy U for $Ca_{1-x}Sr_xWO_4$ ceramics.

x	Lattice energy U(kJ mol^{-1})		
	Ca-O(1)	Ca-O(2)	W-O
0	2722	2720	29564
0.02	2723	2708	29586
0.04	2719	2706	29601
0.06	2715	2703	29619
0.08	2711	2701	29640
0.10	2707	2699	29667

Table 4
Bond energy for $Ca_{1-x}Sr_xWO_4$ ceramics.

x	Bond energy E(kJ mol^{-1})		
	Ca-O(1)	Ca-O(2)	W-O
0	296.4978	296.1545	602.3109
0.02	296.858	294.8322	603.0710
0.04	296.5685	294.7744	603.4365
0.06	296.2673	294.6916	603.9245
0.08	296.0304	294.6965	604.6275
0.10	295.8705	294.3736	605.3934

Table 5
The microwave dielectric properties of $Ca_{1-x}Sr_xWO_4$ ceramics.

x	ε_r	$Q\times f_0$ (GHz)	τ_f (ppm/ °C)
0	10.24	74897	− 24.5
0.02	9.89	76840	− 22.3
0.04	9.76	78011	− 21.3
0.06	9.59	78832	− 20.1
0.08	9.42	79876	− 18.8
0.10	9.27	78917	− 17.7

$$U_{cal} = \sum_{\mu} U_b^{\mu} \tag{9}$$

$$U_b^{\mu} = U_{bc}^{\mu} + U_{bi}^{\mu} \tag{10}$$

$$U_{bc}^{\mu} = 2100m\frac{(Z_+^{\mu})^{1.64}}{(d^{\mu})^{0.75}}f_c^{\mu} \tag{11}$$

$$U_{bi}^{\mu} = 1270\frac{(m+n)Z_+^{\mu}Z_-^{\mu}}{d^{\mu}}\left(1-\frac{0.4}{d^{\mu}}\right)f_i^{\mu} \tag{12}$$

where Z_+^{μ} and Z_-^{μ} are cationic and anionic part presented in μ bond valence respectively; d^{μ} is the chemical bond length of μ bond; f_i^{μ} and f_c^{μ} are the ionic and covalent of the type μ bonds.

The calculation results of lattice energy of $Ca_{1-x}Sr_xWO_4$ ceramics is shown in Table 3.

3.3.4. Calculation of the bond energy

Bond energy can influence the system stability. The bond length and electronegativity are important parameters to obtain the bond energy [16–19]. Zhang et al. have generalized the Sanderson theory and complex theory [3,20]. The bond energy E is composed of two parts, ionic energy E_i^{μ} and covalence energy E_c^{μ}.

$$E = \sum_{\mu} E_b^{\mu} \tag{13}$$

$$E_b^{\mu} = t_c E_c^{\mu} + t_i E_i^{\mu} \tag{14}$$

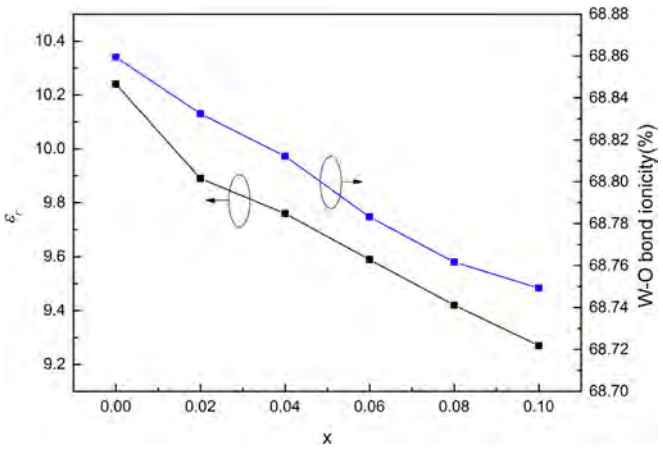

Fig. 4. Dielectric constant and W-O bond ionicity of $Ca_{1-x}Sr_xWO_4$ ($0 \le x \le 0.10$) ceramics.

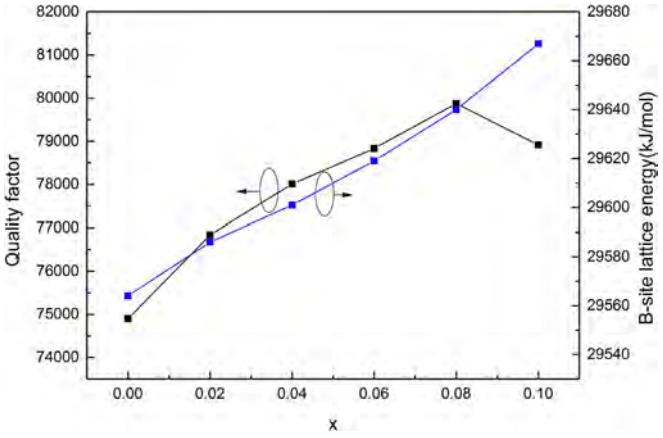

Fig. 5. The $Q\times f_0$ and B-site lattice energy $U_{W\text{-}O}$ of $Ca_{1-x}Sr_xWO_4$ ($0 \le x \le 0.10$) ceramics.

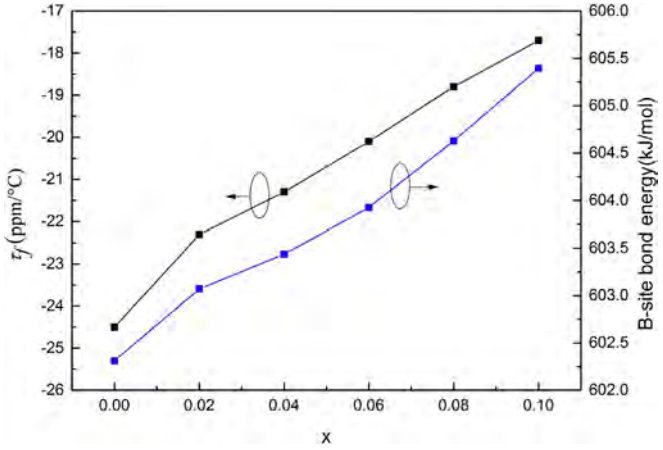

Fig. 6. τf and B-site bond energy of $Ca_{1-x}Sr_xWO_4$ ($0 \le x \le 0.10$) ceramics.

$$E_i^{\mu} = \frac{33200}{d^{\mu}} \tag{15}$$

$$E_c^{\mu} = \frac{(r_{CA} + r_{CB})}{d^{\mu}}(E_{A-A}E_{B-B})^{\frac{1}{2}} \tag{16}$$

$$t_i + t_c = 1 \tag{17}$$

where r_{cA} and r_{cB} are the covalent radii of the ions at A or B site in $CaWO_4$, E_{A-A} and E_{B-B} are the homonuclear bond energy that can be obtained from the handbook, t_c and t_i represent the covalent and ionic blending coefficients, respectively. Here, $r_{cCa} = 171$ p.m., $r_{cW} = 137$ p.m., $r_{cSr} = 185$ p.m., $r_{cO} = 63$ p.m. $E_{Ca\text{-}Ca} = 16.52\ kJ\ mol^{-1}$, $E_{Sr\text{-}Sr} = 16.64\ kJ\ mol^{-1}$ [21]. The results of the bond energy are shown in Table 4.

3.4. Discussion of microwave properties

The microwave dielectric properties of $Ca_{1-x}Sr_xWO_4$ ($0 \le x \le 0.10$) ceramics are illustrated in Table 5. From Table 5 we can see that with the increase of Sr^{2+} dielectric constant decreases, quality factor increases first and then decreases, and temperature coefficient of resonant frequency shifts for the positive direction. The relationship among microwave dielectric properties, bond ionicity, lattice energy and bond energy were discussed.

3.4.1. Dielectric constant

The dielectric constant of ceramic is mainly influenced by second phase and polarizabilities [22]. In this paper, because no second phase was observed, ionic polarizabilities is considered to be the dominant factor [23,24]. In microwave ceramics, ionic polarizabilities can affect the dielectric constant and the ionic polarizability is proportional to bond ionicity. So there should be an intrinsic link between bond ionicity and dielectric constant.

The relationship between dielectric constant and bond ionicity is shown as the following formula:

$$\varepsilon_r = \frac{n^2 - 1}{1 - f_i} + 1 \tag{18}$$

where n is the refractive index.

According to the Eq. (18), we found that the smaller the bond ionicity, the smaller the value of ε_r. The relationship between ε_r and f_i is shown in Fig. 4, from which we can see that the changing trends of dielectric constant and the W-O bond ionicity are similar. With the increase of Sr^{2+} substitution amount, the W-O bond ionicity and the dielectric constant all decreased, revealing the intrinsic link between ε_r and f_i.

3.4.2. Quality factor

The quality factor $Q \times f_0$ is influenced by intrinsic loss and extrinsic loss. The extrinsic loss is influenced by second phases, densification and porosity [25,26], while the intrinsic loss is mainly dominated by lattice vibration modes [27]. Sanderson had reported that, for density sintered samples, the $Q \times f_0$ value had close relationship with B-site lattice energy, the higher B-site lattice energy, the higher the $Q \times f_0$ value [17].

The relationship between quality factor and B-site lattice energy of $Ca_{1-x}Sr_xWO_4$ ($0 \le x \le 0.10$) ceramics is shown in Fig. 5. In this paper, when $x \le 0.08$, the samples were well-sintered and no second phase formed, the value of quality factor was mainly influenced by the intrinsic loss. The $Q \times f_0$ value and B-site lattice energy have a similar increase trend with the increase of Sr^{2+} substitution amount. However, when $x = 0.10$, pores are found in the SEM photographs. Although the B-site lattice energy increase with $x = 0.10$, $Q \times f_0$ value dropped.

3.4.3. Temperature coefficient of resonant frequency

Reaney reported that the structural characteristics of the oxygen polyhedron have a close relationship with the temperature coefficient of resonant frequency. The higher bond energy means the higher restoring force affected on the oxygen polyhedron and the system would be more stable [28].

The changing trend of τ_f and B-site bond energy with the amount of substitution of Sr^{2+} is shown in Fig. 6. With the increase of Sr^{2+}, B-site bond energy also increased, which means the restoring force increased, the τ_f value shifted for the positive direction.

4. Conclusion

The effect of Sr^{2+} substitution for Ca^{2+} on microwave dielectric properties of $Ca_{1-x}Sr_xWO_4$ ceramics was studied in this paper. The samples of $Ca_{1-x}Sr_xWO_4$ ($0 \le x \le 0.10$) were all densified and no second phase appeared. The substitution of Sr^{2+} caused the decrease of dielectric constant, increase of $Q \times f_0$ and τ_f shifting for the positive direction. For the $Ca_{1-x}Sr_xWO_4$ system, the dielectric constant decreased with the decrease of B-site bond iconicity; When $x \le 0.08$, $Q \times f_0$ increases due to the increase of W-site lattice energy; τ_f values shift to the positive directions as the bond energy of the oxygen tetrahedral increased. And the $Ca_{0.92}Sr_{0.08}WO_4$ ceramic sintered at 1100 °C shows the optimum microwave properties: $\varepsilon_r = 9.42$, $Q \times f_0 = 79876$ GHz and $\tau_f = -18.8$ ppm/°C.

Acknowledgments

This work was supported by the National Natural Science Foundation of China (No. 61671323).

References

[1] L.C. Tien, C.C. Chou, Ordered structure and dielectric properties of lanthanum-substituted Ba ($Mg_{1/3}Ta_{2/3}$) O_3, J. Am. Ceram. Soc. 83 (2000) 2074–2078.
[2] D.W. Kim, D.Y. Kim, Phase relations and microwave dielectric properties of $ZnNb_2O_6$-TiO_2, J. Mater. Res. 15 (2000) 1331–1335.
[3] D. Zhou, L.X. Pang, High permittivity and low loss microwave dielectrics suitable for 5G resonators and low temperature co-fired ceramic architecture, J. Mater. Chem. C. 5 (2017) 10094–10098.
[4] P. Zhang, Y.G. Zhao, The correlations between electronic polarizability, packing fraction, bond energy and microwave dielectric properties of $Nd(Nb_{1-x}Sb_x)O_4$ ceramics, J. Alloy. Compd. 644 (2015) 621–625.
[5] E.S. Kim, B.S. Chun, Effects of packing fraction and bond valence on microwave dielectric properties of $A^{2+}B^{6+}O_4$ (A^{2+}: Ca, Pb, Ba; B^{6+}: Mo, W) ceramics, J. Eur. Ceram. Soc. 30 (2010) 1731–1736.
[6] L. Wang, J.J. Bian, Effect of $Na_2W_2O_7$ addition on low-temperature sintering and microwave dielectric properties of $CaWO_4$, Mater. Lett. 65 (2011) 726–728.
[7] Z. Zhang, H. Su, Glass-free low-temperature sintering and microwave dielectric properties of $CaWO_4$–Li_2WO_4 ceramics, Ceram. Int. 40 (2014) 1613–1617.
[8] M. Xiao, Z.Q. Zhou, Influence of molybdenum substitution on the microwave dielectric properties of $CaWO_4$ ceramic, J. Mater. Sci. Mater. Electron. 28 (2017) 10343–10348.
[9] H.H. Xi, D. Zhou, Raman Spectra, Infrared Spectra, and Microwave Dielectric Properties of Low-Temperature Firing $[(Li_{0.5}Ln_{0.5})_{1-x}Ca_x]$ MoO_4 (Ln = Sm and Nd) Solid Solution Ceramics with Scheelite Structure, J. Am. Ceram. Soc. 98 (2015) 587–593.
[10] P. Zhang, Y.G. Zhao, Bond ionicity, lattice energy, bond energy and microwave dielectric properties of $ZnZr(Nb_{1-x}A_x)_2O_8$ (A = Ta, Sb) ceramics, Dalton Trans. 44 (2015) 16684–16693.
[11] H.W. Lee, J.H. Park, Low-temperature sintering of temperature-stable $LaNbO_4$ microwave dielectric ceramics, Mater. Res. Bull. 45 (2010) 21–24.
[12] J.C. Phillips, Phys. dielectric definition of electronegativity, Phys. Rev. Lett. 20 (1968) 550–553.
[13] J.C. Phillips, J.A. Van Vechten, Dielectric classification of crystal structures, ionization potentials, and band structures, Phys. Rev. Lett. 22 (1969) 705–708.
[14] Z.J. Wu, S.Y. Zhang, Calculation of chemical bond parameters in $La_{1-x}Ca_xCrO_3$ ($0.0 \le x \le 0.3$), Int. J. Quantum Chem. 73 (1999) 433–437.
[15] S.Y. Zhang, Chemical Bond Theory of Complex Structure Crystals on Dielectric Description and application, Science Publisher, Beijing, 2005.
[16] R.T. Sanderson, Bond energies, J. Inorg. Nucl. Chem. 28 (1966) 1553–1565.
[17] R.T. Sanderson, Multiple and single bond energies in inorganic molecules, J. Inorg. Nucl. Chem. 30 (1968) 375–393.
[18] R.T. Sanderson, Chemical Bonds and Bond Energy, Academic Press, New York, 1971.
[19] R.T. Sanderson, Electronegativity and bond energy, J. Am. Chem. Soc. 105 (1983) 2259–2261.
[20] P. Zhang, Y.G. Zhao, Effects of structural characteristics on microwave dielectric properties of $Li_2Mg(Ti_{1-x}Mn_x)_3O_8$ ceramics, J. Alloy. Compd. 647 (2015) 386–391.

[21] Y.R. Luo, Comprehensive Handbook of Chemical Bond Energies, Taylor& Francis Group, LLC, CRC Press, 2007.
[22] E.S. Kim, K.H. Yoon, Microwave dielectric properties of $(1-x)$ $CaTiO_3$–$xLi_{1/2}Sm_{1/2}TiO_3$ ceramics, J. Eur. Ceram. Soc. 23 (2003) 2397–2401.
[23] R.D. Shannon, Dielectric polarizabilities of ions in oxides and fluorides, J. Appl. Phys. 73 (1993) 348–366.
[24] C.L. Huang, S.H. Huang, Low-loss microwave dielectric ceramics in the $(Co_{1-x}Zn_x)TiO_3$ (x = 0–0.1) system, J. Alloy. Compd. 515 (2012) 8–11.
[25] Q.W. Liao, L.X. Li, Structural dependence of microwave dielectric properties of ixiolite structured $ZnTiNb_2O_8$ materials: crystal structure refinement and Raman spectra study, Dalton Trans. 41 (2012) 6963–6969.
[26] D. Zhou, Li.X. Pang, Phase composition and phase transformation in Bi(Sb, Nb, Ta)O_4 system, Solid State Sci. 11 (2009) 1894–1897.
[27] J. Petzelt, S. Pačesová, Dielectric spectra of some ceramics for microwave applications in the range of 10^{10}–10^{14} Hz, Ferroelectrics 93 (1989) 77–85.
[28] I.M. Reaney, E.L. Colla, Dielectric and structural characteristics of Ba-and Sr-based complex perovskites as a function of tolerance factor, Jpn J. Appl. Phys. 33 (1994) 3984–3990.